


**Nonequilibrium liquid-vapor interfaces: Linear and nonlinear descriptions**Henning Struchtrup \**Department of Mechanical Engineering, University of Victoria, Victoria, British Columbia, Canada V8W 2Y2*Hans Christian Öttinger *Quantum Center and Department of Materials, ETH Zürich, HCP F 43.1, CH-8093 Zürich, Switzerland*

(Received 6 September 2023; accepted 8 November 2023; published 1 December 2023)

While it is often assumed that liquid-vapor interfaces in nonequilibrium processes are in states of local thermodynamic equilibrium, this might not be the case for strong deviations from equilibrium. Clausius-Clapeyron equations for bulk properties yield a consistently defined temperature of the interface that is close to the liquid bulk temperature. The alternative interface temperature defined through the surface tension will be different for stronger nonequilibrium processes. Structural variables are introduced to extend the thermodynamic description of interfaces to a wider range of processes. Interfacial resistivities will depend on interface temperature as well as mass and heat flux through the interface.

DOI: [10.1103/PhysRevE.108.064801](https://doi.org/10.1103/PhysRevE.108.064801)**I. INTRODUCTION**

While evaporation of liquids and condensation of vapors are processes of daily experience, as well as commonly employed in technical systems such as vapor power plants or refrigerators and heat pumps, some finer details of these processes are still surprisingly little understood. In this contribution, we discuss the thermodynamic description of liquid-vapor interfaces in nonequilibrium heat and mass transfer processes.

As a typical setting, Fig. 1 shows one-dimensional transport through a plane interface separating liquid (L) and vapor (V). Motion of the interface is relative to the observer. For the discussion of interfacial behavior, the viewpoint of an observer resting relative to the interface is most convenient, and the figure and the subsequent equations are for such an observer. Due to nonequilibrium enforced by suitable boundary conditions, mass flux  $J$  and energy flux  $Q$  pass through the interface, where the fluxes entering and leaving might be different in the case of mass or energy accumulation or depletion in the interface. Typical Mach numbers are low; thus both phases are at the same pressure.

Theoretical evaluation [1–3] as well as experiments [4–7] yield finite temperature differences  $\Delta T = T_V - T_L$  between liquid and vapor on both sides of the interface, and deviations of pressure  $p$  from equilibrium saturation pressure  $p_{\text{sat}}$ . As interface effects, these jumps are mostly visible in smaller, i.e., microscopic, systems, where interface resistances contribute more to overall system resistance than in macroscopic

systems. Nevertheless, significant temperature jumps were reported for systems on the centimeter scale [6,7].

The thermodynamic description of these jumps is through interface relations that introduce coefficients to describe the transport behavior, the so-called interface resistivities [2]. From the particle viewpoint of kinetic theory of gases, the interface behavior is given through condensation and accommodation coefficients, so that resistivities are expressed through these [1–3]. In any case, the coefficients describing the interface are introduced from theoretical considerations and cannot be found from first principles. That is, one always faces the need to determine resistivities or condensation and accommodation coefficients from suitable experiments.

Physical experiments at macroscopic scales in the laboratory are typically conducted in steady state, where vapor is removed by a vacuum pump, while liquid is replaced such that the interface remains stationary, while the temperatures of the liquid and vapor boundaries are fixed [6,7]. Evaluation of measurements suffers from significant experimental errors; notably the error in pressure measurement is at least as large as the expected experimental deviation from saturation pressures [7,8]. Typical experiments are restricted to relatively low evaporation and heat fluxes close to the triple point.

Molecular dynamics (MD) simulations offer an alternative, where small systems can be studied at full resolution of the interface, with well-controlled process parameters such as evaporation mass flux, temperature gradients in the bulk phases, etc. Simulations typically mimic the experimental setting with stationary interface, vapor particles removed and reinjected into the liquid, and thermostatted liquid and vapor regions at the boundaries.

In order to extract meaningful data above the stochastic noise, MD simulations are typically run at rather strong nonequilibrium conditions, with large evaporation fluxes and steep temperature gradients [9–16].

\*struchtr@uvic.ca; <http://www.engr.uvic.ca/struchtr/>

*Published by the American Physical Society under the terms of the Creative Commons Attribution 4.0 International license. Further distribution of this work must maintain attribution to the author(s) and the published article's title, journal citation, and DOI.*

MD simulations resolve the molecular scale and yield a diffuse interface with a continuous change of mass density over a few molecular diameters, and temperature and velocity Knudsen layers in the vapor with thickness of the order of the mean-free path. However, the main interest is for sharp interface models for larger scales, where the interface is not resolved, and described by the coefficients mentioned above, which thus account for effects in the interface itself and in the Knudsen layers. Finding these coefficients requires extrapolations of the MD data and careful evaluation of interface conditions. This procedure also leads to the question of how the (sharp) interface must be characterized.

In an extension of Gibbs' theory for equilibrium interfaces, Bedeaux and coworkers proposed a local equilibrium description, where the interface is an autonomous thermodynamic element with its own temperature  $T_s$  [17]. Gauge invariance of the interface location yields an extension to nonequilibrium of Clausius-Clapeyron-style relations found by Gibbs for equilibrium interfaces [18]; see [19] for a thorough presentation. The consistency of the local equilibrium model for the phase interface was reported in simulations for a square gradient model [17,20], as well as for molecular dynamics simulations of a single substance [11] and of mixtures [16].

Typically thermodynamic descriptions of nonequilibrium interface rely on the ideas of linear irreversible thermodynamics (LIT) [2,19], which assumes linear relations between thermodynamic (mass and energy) fluxes and their thermodynamic forces, which here are deviations in chemical potentials and temperatures from equilibrium. In LIT, interface resistivities relate forces and fluxes through linear relations, where the resistivities depend only on the suitably defined interface temperature.

Sharp interface models in kinetic theory yield the celebrated Hertz-Knudsen-Schrage model and its variants [3,21–25], which yield nonlinear expressions between mass and energy fluxes and the thermodynamic driving forces (a model of this kind is briefly presented and discussed in the Appendix). Furthermore, recent evaluations of a moment model for the Enskog-Vlasov equation [26,27] indicate nonlinearity between forces and fluxes for larger mass fluxes.

Thus, kinetic theory results suggest flow regimes for evaporation and condensation processes in stronger nonequilibrium, i.e., large mass and energy fluxes, where the linear relations of LIT cease to hold. To embed these processes into thermodynamics, this contribution explores liquid-vapor interfaces in the linear and nonlinear regimes.

Specifically, it will be shown that the definition of interface temperature from two Clausius-Clapeyron-style equations [17–19] results directly from the bulk properties of the two phases in the linear limit, hence this interface temperature is not linked to any specific properties of the interface itself. Numerical evaluation for simple two-phase property relations shows that the such a defined interface temperature is rather close to the temperature of the liquid at the interface. Another definition of interface temperature through the surface tension appears to be independent from this.

Then, in order to include nonlinear effects in the thermodynamic description of the interface, we introduce structural (or internal) nonequilibrium variables. This extended interface model yields the same conditions for gauge invariance, and

thus the same interface temperature than the simpler model. Application of LIT leads to resistivities that depend not only on interface temperature but also on the structural variables.

Due to their smallness, nonequilibrium liquid-vapor interfaces will most often be met in steady state. In this limit the extended transport model reduces to the typical LIT description, where the resistivities are expressed through the extended resistivities, and thus depend on interface temperature and structural variables. As well, in steady state structural variables are linked to mass and energy fluxes, hence the steady-state resistivities depend on the fluxes through the structural variable. With this, the steady-state reduction of the LIT model with structural variables results in a nonlinear modification of the usual LIT expressions for the interface, with resistivities that depend on temperature and mass and energy fluxes through the interface.

The remainder of the paper proceeds as follows. To set the stage, in Sec. II we recall the description of phase equilibrium between bulk liquid and vapor and the interface, formulate Gibbs, Euler, and Gibbs-Duhem equations, and from these the Clausius-Clapeyron-style interface relations. We show the latter result as well from the requirement of gauge invariance.

Section III presents the extension of the equilibrium description to interfaces in local thermodynamic equilibrium, with three possible definitions for interface temperature, one from surface tension and two from Clausius-Clapeyron relations. Using thermodynamic relations for the bulk phases, we show that these agree within first-order differences between bulk liquid and vapor states. These relations are further used to evaluate the expected interface temperature  $T_s$  for two simple liquid-vapor models (van der Waals, Carnahan-Starling-Sutherland), where it is found that the so-defined interface temperature will be close to the temperature  $T_L$  of the bulk liquid at the interface. The section closes with a qualitative discussion of differences with the temperature defined from surface tension.

The model with structural variable(s) is developed and examined in Sec. IV. Gibbs, Euler, and Gibbs-Duhem relations are extended by terms accounting for the additional variable. The further evaluation shows that the Clausius-Clapeyron-style equations remain unchanged and give the same interface temperature  $T_s$  as before. Surface tension, however, is affected by the structural variable, which therefore serves to distinguish the definitions of interface temperature.

The Gibbs equation forms the base for the development for a 1D transport model for heat and mass transfer through the interface, consisting of conservation laws for interfacial mass, energy, and the structural variable. Following the usual steps of LIT, the entropy balance results from combining these with the Gibbs equation, and entropy generation is identified as a product of thermodynamic forces and fluxes. Further following LIT, force-flux relations for the interface are identified. These can be reduced to the usual form encountered for steady-state interfaces, where the reduction of the full model now shows that the resistivity coefficients will depend on the interface temperature and heat and mass fluxes.

The paper ends with our conclusions. Further evaluation of nonlinear resistivities is underway and will be presented elsewhere. Nevertheless, for better appreciation of the ideas

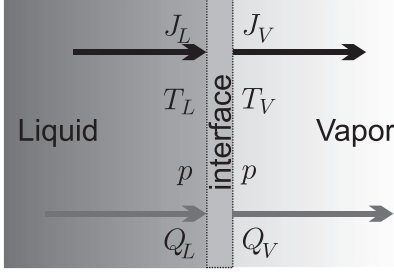


FIG. 1. Liquid-vapor interface in nonequilibrium, with mass flux  $J$  and energy flux  $Q$  passing through the interface. In this nonequilibrium process, liquid and vapor temperatures  $T_L, T_V$  at the interface differ. Both phases are at the same pressure  $p$ , which differs from saturation pressures  $p_{\text{sat}}(T_L)$  and  $p_{\text{sat}}(T_V)$ . In steady state  $J_L = J_V = J$  and  $Q_L = Q_V = Q$ .

developed, the Appendix shows that the classical Hertz-Knudsen-Schrage model is naturally nonlinear and will be a good start for further exploration.

## II. EQUILIBRIUM STATES

### A. Bulk phases

We are interested in an interface separating a simple liquid (L) from its vapor (V); see Fig. 1.

In thermodynamic equilibrium states the system exhibits homogeneous temperature  $T$ , homogeneous pressure equal to saturation pressure  $p_{\text{sat}}(T)$ , and homogeneous chemical potential (or mass specific Gibbs free energy)  $\mu_E(T) = u + \frac{p}{\rho} - Ts$  (specific internal energy  $u$ , mass density  $\rho$ , and specific entropy  $s$ ), while mass and heat fluxes vanish. Thus, in equilibrium liquid and vapor bulk properties are related as [28]

$$\begin{aligned} T_L &= T_V = T, \\ p_L &= p_V = p_{\text{sat}}(T), \\ \mu_L(T, p_{\text{sat}}(T)) &= \mu_V(T, p_{\text{sat}}(T)) = \mu_E(T). \end{aligned} \quad (1)$$

We denote densities of energy and entropy as  $\varepsilon = \rho u$ ,  $\eta = \rho s$  and write the corresponding Gibbs and Gibbs-Duhem equations as [19]

$$Td\eta = d\varepsilon - \mu d\rho, \quad dp = \eta dT + \rho d\mu, \quad (2)$$

while the definition of chemical potential gives the Euler equation

$$-p = \varepsilon - T\eta - \rho\mu. \quad (3)$$

Taking the difference for the last two equations between liquid and vapor phases in equilibrium at  $T, p_{\text{sat}}, \mu_E$ , we find, with the notation  $\Delta\phi = \phi_V - \phi_L$ ,

$$0 = \Delta\varepsilon_{\text{sat}} - T\Delta\eta_{\text{sat}} - \mu_E\Delta\rho_{\text{sat}}, \quad 0 = \Delta\eta_{\text{sat}}dT + \Delta\rho_{\text{sat}}d\mu_E, \quad (4)$$

which gives Clausius-Clapeyron-style equations for equilibrium states,

$$\begin{aligned} \frac{\Delta\varepsilon}{\Delta\rho} \Big|_{\text{sat}} &= \frac{d\frac{\mu_E}{T}}{d\frac{1}{T}} \\ \frac{\Delta\eta}{\Delta\rho} \Big|_{\text{sat}} &= -\frac{d\mu_E}{dT}. \end{aligned} \quad (5)$$

These equations relate differences of properties between vapor and liquid to the equilibrium chemical potential  $\mu_E(T)$ ; the subscript ‘‘sat’’ emphasizes that these relations are valid for saturated equilibrium states.

### B. Interface excess properties

For a two-phase system with interface, the Gibbs equation requires a term accounting for the work in increasing interfacial area  $A$ , which is given by (equilibrium) surface tension  $\gamma_E(T)$  as

$$dU = TdS - pdV + \mu_E dm + \gamma_E dA. \quad (6)$$

Since the equilibrium state is a function only of temperature, the interfacial tension in equilibrium is a function only of temperature.

This gives rise to the Euler and Gibbs-Duhem relations for the full system of bulk phases plus interface as

$$\begin{aligned} G &= U + pV - TS - \gamma_E A \\ 0 &= -SdT + Vdp - md\mu_E - Ad\gamma_E, \end{aligned} \quad (7)$$

with total Gibbs free energy  $G$ . For each bulk phase ( $\alpha = L, V$ ), we have  $G_\alpha = U_\alpha + pV_\alpha - TS_\alpha$ ,  $0 = -S_\alpha dT + V_\alpha dp - m_\alpha d\mu_E$ , and subtracting these from the equations for the system gives the corresponding equations for the interface. After division by surface area  $A$ , and assuming that the interface does not contribute to volume so that  $V_L + V_V = V$ , we find Euler and Gibbs-Duhem equations for the equilibrium interface as

$$\mu_E \rho_s = \varepsilon_s - T\eta_s - \gamma_E, \quad 0 = -\eta_s dT - \rho_s d\mu_E - d\gamma_E, \quad (8)$$

where all properties with subscript  $s$  are surface densities, e.g.,  $\rho_s = (m - m_L - m_V)/A$ , etc. Combination of the two equations (8) results in the Gibbs equation for the interface,

$$Td\eta_s = d\varepsilon_s - \mu_E d\rho_s. \quad (9)$$

Considering a microscopic look at the interface, it is smooth, in particular with a smooth curve for mass density  $\tilde{\rho}(x)$  between equilibrium bulk states  $\rho_L, \rho_V$ . In sharp interface modeling we take a macroscopic viewpoint, with a sharp jump between the bulk phases; that is, bulk properties are extrapolated to a point  $x_0$  within the interface. The interfacial properties can then be considered as the excess properties that result from the difference between the actual and extrapolated curves. The excess mass density is defined as

$$\rho_s(x_0) = \int_{x_0-L}^{x_0} (\tilde{\rho}(x) - \rho_L) dx + \int_{x_0}^{x_0+L} (\tilde{\rho}(x) - \rho_V) dx, \quad (10)$$

where the domain length  $L$  is sufficiently large so that the integrands vanish outside the interval  $(x_0 - L, x_0 + L)$ ; see Fig. 2.

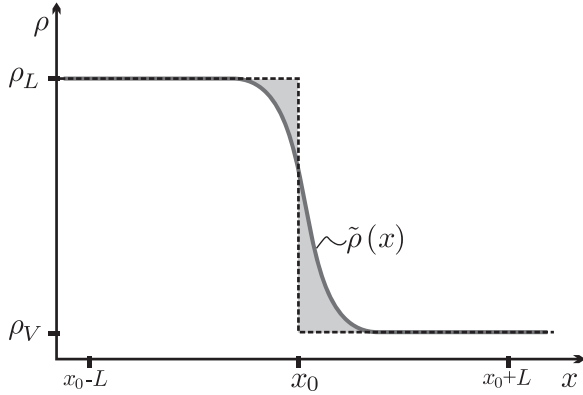


FIG. 2. Smooth mass density curve  $\tilde{\rho}(x)$  (grey) and sharp interface model  $(\rho_L, \rho_V)$  (dashed) with interface location  $x_0$ . The difference between the gray areas is the excess density  $\rho_s(x_0)$ .

For simplicity, the figure shows a monotonous density curve. For temperatures below the Fisher-Widom line, on the liquid side the density exhibits oscillations on the molecular scale which decay towards the bulk liquid [29–31]. The domain length  $L$  must be chosen such that the oscillations decay within the interval.

The excess density in Eq. (10) and Fig. 2 is defined as the difference of two contributions. The gauge transformation behavior results entirely from the subtraction of the sharp-interface contribution through the arbitrariness of the location of the sharp interface. For an excess density and its gauge-transformation behavior it is not essential that the actual contribution can be calculated from a smooth profile. Such a smooth profile may not exist for nonlocal properties, such as entropy. However, even for a nonlocal extensive quantity, one can define an excess density that obtains the proper gauge-transformation behavior from the subtracted sharp-interface contribution.

Obviously, the value of the excess density depends on the chosen location  $x_0$  of the so-called dividing surface [18,19], and a gauge transformation; i.e., a shift of size  $l$  in that location results in shifted values for the surface densities,

$$\begin{aligned}\rho_s(x_0 + l) &= \rho_s(x_0) + \Delta\rho l, \\ \varepsilon_s(x_0 + l) &= \varepsilon_s(x_0) + \Delta\varepsilon l, \\ \eta_s(x_0 + l) &= \eta_s(x_0) + \Delta\eta l.\end{aligned}\quad (11)$$

Temperature  $T$ , surface tension  $\gamma_E$ , and chemical potential  $\mu_E$  are intensive properties of the equilibrium state and hence invariant against these shifts.

Taking the shifted Euler equation (8)<sub>1</sub> we find

$$\begin{aligned}\rho_s(x_0)\mu_E &= \varepsilon_s(x_0) - T\eta_s(x_0) - \gamma_E \\ &+ [\Delta\varepsilon - T\Delta\eta + \mu_E\Delta\rho]l.\end{aligned}\quad (12)$$

We have to address two possible viewpoints on this equation. Coming from phase equilibrium for the bulk phases, we know that for a single phase  $(\varepsilon_\alpha - T\eta_\alpha + \rho_\alpha\mu) = -p$ , hence the shift term becomes  $[-\Delta p] \cdot l = 0$ , since in equilibrium temperature and chemical potential are homogenous, and the bulk pressures are identical [and equal to  $p_{sat}(T)$ ]. With this, we conclude that the Euler equation for the interface is

independent of the chosen location of the dividing surface—the Euler equation is invariant against gauge transformations.

Alternatively, one can demand that the Euler equation is invariant, which results in the requirement

$$\Delta\varepsilon - T\Delta\eta + \mu_E\Delta\rho = 0. \quad (13)$$

As well, demanding gauge invariance of the Gibbs-Duhem equation (8)<sub>2</sub> gives

$$0 = -\Delta\eta dT - \Delta\rho d\mu_E. \quad (14)$$

With this argument, the Clausius-Clapeyron equations (5) result from the demand for invariance of the thermodynamic description of the interface against gauge transformations.

Independent of the viewpoint, from Euler and Gibbs-Duhem equation we find directly

$$\eta_s(T) = -\frac{d\gamma_E}{dT} - \rho_s\frac{d\mu_E}{dT}, \quad \varepsilon_s(T) = \frac{d\gamma_E}{dT} + \rho_s\frac{d\mu_E}{dT}, \quad (15)$$

so that—maybe not surprisingly—all (equilibrium) surface densities depend on the chosen location of the dividing surface through the choice of the surface mass density  $\rho_s$ . The most convenient choice is the gauge  $\rho_s = 0$ , the equimolar surface, where surface entropy and energy are directly related to surface tension,

$$\eta_s(T) = -\frac{d\gamma_E}{dT}, \quad \varepsilon_s(T) = \frac{d\gamma_E}{dT}. \quad (16)$$

Note that  $\gamma_E(T)$  and  $\mu_E(T)$  are functions of temperature only; hence in equilibrium also interfacial entropy  $\eta_s$  and energy  $\varepsilon_s$  are functions of temperature alone. Inserting the above expressions for  $\eta_s$  and  $\varepsilon_s$  into the Gibbs equation (9) results in an identity.

### III. NONEQUILIBRIUM PROCESSES WITH LOCAL EQUILIBRIUM INTERFACE

#### A. Postulates

Classical nonequilibrium thermodynamics postulates local equilibrium states in bulk phases [2,19], that is, it assumes the local validity of thermal and caloric equations of state and Gibbs equation.

In this context we note that in the small systems that naturally occur in resolved descriptions of interfaces, thermodynamic properties may depend on underlying statistical ensembles. Here, however, we consider only profiles of well-defined mechanical properties. As long as we do not consider profiles of entropy (or any other properties that can be defined only for many-particle systems), ensemble dependence is not an issue [32–34].

The evaluation of the postulates leads to the well-known Navier-Stokes-Fourier (NSF) equations to describe processes in not too strong nonequilibrium. Comparison with experiments gives validation of the postulates.

On the other hand, within kinetic theory of gases one derives the NSF equations from the Chapman-Enskog method, which confirms what was postulated before, i.e., validity of local equations of state and Gibbs equations result from Chapman-Enskog expansion to first order [35].

With local equilibrium of bulk phases well understood, one will consider extending the assumption of local equilibrium to phase interfaces, such that the interface itself is in local equilibrium, but not in equilibrium with the adjacent bulk phases. Then the relations (8) of the previous section should remain valid, where now all interface properties depend on interface temperature  $T_s$ , which must be allowed to be different from the temperatures  $T_L, T_V$  of the bulk phases at the interface.

For the following, we must be clear on notation. In general nonequilibrium processes, thermodynamic properties exhibit nonhomogeneous values in the bulk phases adjacent to the interface region of finite but rather small thickness. The location of the dividing surface lies somewhere within the interfacial region, and thermodynamic properties values are extrapolated from the respective bulk phases to the location of the dividing surface.

In the following, the indices  $L, V$  refer to the values of thermodynamic properties at either side of the dividing surface, *as they result from extrapolation*. For instance,  $T_L, T_V$  are the extrapolated values of liquid and vapor temperatures, and  $\Delta T = T_V - T_L$  is the temperature jump across the dividing surface. Note that in equilibrium bulk properties are homogeneous, hence this notation is agreeable with our description of phase equilibrium, where extrapolated values agree with the homogeneous bulk values.

The assumption of a local equilibrium temperature  $T_s$  of the interface requires a rational method of determination. As in equilibrium, the exact location of the dividing surface must play no role; that is, also in the local equilibrium case, Eqs. (8)—which remain valid in the local equilibrium state—must be invariant against a shift in the dividing surface. Moreover, the surface tension, which is—at least in principle—a measurable property of the interface, should be the same function of temperature as in equilibrium.

With that, one finds three conditions linking measurements of (extrapolated) bulk properties  $\rho, \varepsilon, \eta$  and surface tension  $\gamma$  in nonequilibrium to the proposed local equilibrium interface temperature  $T_s$ ,

$$\frac{\Delta\eta}{\Delta\rho} = - \left. \frac{d\mu_E(T)}{dT} \right|_{T=T_s^{(\eta)}}, \quad \frac{\Delta\varepsilon}{\Delta\rho} = \left. \frac{d\frac{\mu_E(T)}{T}}{d\frac{1}{T}} \right|_{T=T_s^{(\varepsilon)}},$$

$$\gamma = \gamma_E(T_s^{(\gamma)}). \quad (17)$$

Here  $\Delta\eta, \Delta\varepsilon, \Delta\rho$  are differences of bulk properties in nonequilibrium, extrapolated to the dividing surface. On the right-hand side of these equations,  $\gamma_E(T_s)$  and  $\mu_E(T_s)$  are surface tension and chemical potential of the equilibrium state at temperature  $T_s$ .

Further evaluation of these relations requires explicit equations of state and numerical evaluation; see Sec. III C.

The postulate of local interfacial equilibrium states that the three relations above, with given values for the nonequilibrium state differences on the left-hand side, yield the same interface temperature,

$$T_s = T_s^{(\eta)} = T_s^{(\varepsilon)} = T_s^{(\gamma)}. \quad (18)$$

In the next subsections we show that the first two conditions yield the same interface temperature as long as the bulk deviation from the saturation state at  $T_s = T_s^{(\eta)} = T_s^{(\varepsilon)}$  is of

first order, which is typically the case for evaporation and condensation processes at low Mach numbers. It will also be seen that  $T_s$  is rather close to the temperature  $T_L$  of the liquid at the interface.

From a thermodynamic perspective, the interfacial temperature is not a stand-alone quantity and should be defined such that it comes with an interfacial entropy as a conjugate partner. At equilibrium, we know from Gibbs' theory that the excess entropy is deeply related to the interfacial tension, which, as a function of temperature, actually serves as a thermodynamic potential for the interfacial thermodynamics. Therefore, defining nonequilibrium interfacial temperature in terms of interfacial tension provides a natural generalization.

At present, we are not aware of a link between the interface temperature that follows from surface tension  $T_s^{(\gamma)}$  and the interface temperature  $T_s^{(\eta)} = T_s^{(\varepsilon)}$  from the bulk jumps. Equality of both remains a postulate. MD simulations give some evidence that the two temperatures are not too different [11,16,17,20], while a recent evaluation of a van der Waals model finds significant differences [32].

## B. Jump ratios and interfacial temperature

We consider the ratios  $\frac{\Delta\eta}{\Delta\rho}, \frac{\Delta\varepsilon}{\Delta\rho}$  for a nonequilibrium state not too far from an equilibrium state at  $T_s$ . Note that the temperature  $T_s$  is to be determined. To proceed, we denote the deviation of bulk properties ( $\alpha = L, V$ ) from the saturated equilibrium state at  $T_s$  as, for a generic property  $\phi$ ,

$$\phi_\alpha = \phi_{\alpha,\text{sat}}(T_s) + \delta\phi_\alpha. \quad (19)$$

We consider all equations to first order in the deviations  $\delta\phi_\alpha$ , and denote  $\Delta\delta\phi = \delta\phi_V - \delta\phi_L$ .

For the differences of bulk properties at the interface we find for densities of mass and energy

$$\Delta\rho = \Delta\rho_{\text{sat}} \left( 1 + \frac{\Delta\delta\rho}{\Delta\rho_{\text{sat}}} \right), \quad \Delta\varepsilon = \Delta\varepsilon_{\text{sat}} \left( 1 + \frac{\Delta\delta\varepsilon}{\Delta\varepsilon_{\text{sat}}} \right), \quad (20)$$

and for entropy density, with the help of the Taylor expansion and Gibbs equation (2),

$$\Delta\eta = \Delta\eta_{\text{sat}} \left( 1 + \frac{1}{T_s} \frac{\Delta\delta\varepsilon}{\Delta\eta_{\text{sat}}} - \frac{\mu_E(T_s)}{T_s} \frac{\Delta\delta\rho}{\Delta\eta_{\text{sat}}} \right); \quad (21)$$

here  $T_s$  and  $\mu_E(T_s)$  appear under the assumption that the  $\delta\rho_\alpha, \delta\varepsilon_\alpha$  are sufficiently small.

From the above, to leading order in the  $\Delta\delta\phi$  the ratios (17) can be written as

$$\frac{\Delta\eta}{\Delta\rho} = \left. \frac{\Delta\eta}{\Delta\rho} \right|_{\text{sat}, T_s} \left( 1 + \frac{1}{T_s} \frac{\Delta\delta\varepsilon}{\Delta\eta_{\text{sat}}} - \frac{\mu_E(T_s)}{T_s} \frac{\Delta\delta\rho}{\Delta\eta_{\text{sat}}} - \frac{\Delta\delta\rho}{\Delta\rho_{\text{sat}}} \right), \quad (22)$$

$$\frac{\Delta\varepsilon}{\Delta\rho} = \left. \frac{\Delta\varepsilon}{\Delta\rho} \right|_{\text{sat}, T_s} \left( 1 + \frac{\Delta\delta\varepsilon}{\Delta\varepsilon_{\text{sat}}} - \frac{\Delta\delta\rho}{\Delta\rho_{\text{sat}}} \right), \quad (23)$$

where  $\left. \frac{\Delta\eta}{\Delta\rho} \right|_{\text{sat}, T_s}, \left. \frac{\Delta\varepsilon}{\Delta\rho} \right|_{\text{sat}, T_s}$  are given by (5) evaluated at  $T_s$ . To have  $T_s$  in agreement with the postulate of local equilibrium

(17), the terms in both brackets must simultaneously reduce to unity:

$$\frac{1}{T_s} \frac{\Delta \delta \varepsilon}{\Delta \eta_{\text{sat}}} - \frac{\mu_E(T_s)}{T_s} \frac{\Delta \delta \rho}{\Delta \eta_{\text{sat}}} - \frac{\Delta \delta \rho}{\Delta \rho_{\text{sat}}} = 0, \quad (24)$$

$$\frac{\Delta \delta \varepsilon}{\Delta \varepsilon_{\text{sat}}} - \frac{\Delta \delta \rho}{\Delta \rho_{\text{sat}}} = 0. \quad (25)$$

From the second equation (25) this is the case if

$$\Delta \delta \varepsilon = \frac{\Delta \varepsilon_{\text{sat}}}{\Delta \rho_{\text{sat}}} \Delta \delta \rho, \quad (26)$$

while the Euler equation (3) in equilibrium yields

$$\varepsilon_{\alpha, \text{sat}}(T_s) - T_s \eta_{\alpha, \text{sat}}(T_s) - \rho_{\alpha, \text{sat}}(T_s) \mu_E(T_s) = -p_{\text{sat}}(T_s). \quad (27)$$

Combining all of the above, we find for the first condition (24)

$$\begin{aligned} 0 &= \frac{1}{T_s} \frac{\Delta \delta \varepsilon}{\Delta \eta_{\text{sat}}} - \frac{\mu_E(T_s)}{T_s} \frac{\Delta \delta \rho}{\Delta \eta_{\text{sat}}} - \frac{\Delta \delta \rho}{\Delta \rho_{\text{sat}}} \\ &= \frac{\Delta \delta \rho}{T_s \Delta \rho_{\text{sat}} \Delta \eta_{\text{sat}}} [\Delta \varepsilon_{\text{sat}} - T_s \Delta \eta_{\text{sat}} - \mu_E(T_s) \Delta \rho_{\text{sat}}] = 0, \end{aligned} \quad (28)$$

so that both equations are simultaneously fulfilled, i.e., the temperatures from the jump conditions agree:  $T_s^{(\eta)} = T_s^{(\varepsilon)} = T_s$ .

### C. Evaluation of jump conditions

It is interesting to have a closer look at the differences between the bulk temperatures  $T_L$ ,  $T_V$  and the proposed interface temperature  $T_s$  obtained from the jump conditions. By expansion around the equilibrium state at  $T_s$  we can write (22) to leading order in the alternative form

$$\frac{\Delta \eta}{\Delta \rho} = \frac{\Delta \eta}{\Delta \rho} \Big|_{\text{sat}, T_s} \left( 1 + \alpha_{T_L} \frac{\delta T_L}{T_s} + \alpha_{\Delta T} \frac{\Delta T}{T_s} + \alpha_p \frac{\delta p}{p_{\text{sat}}(T_s)} \right). \quad (29)$$

Here we introduced the bulk temperature difference  $\Delta T = T_V - T_L = \delta T_V - \delta T_L$ , which can be measured;  $\delta p = p - p_{\text{sat}}(T_s)$  is the deviation of the common bulk pressure ( $p = p_L = p_V$ ) from saturation at  $T_s$ . The ratios  $\frac{\delta T_L}{T_s}$ ,  $\frac{\Delta T}{T_s}$ ,  $\frac{\delta p}{p_{\text{sat}}(T_s)}$  are obvious smallness parameters; in a linear theory their absolute values should be below 0.05 (e.g., this is so for Ward's experiments with water). The coefficients  $\alpha_{T_L}$ ,  $\alpha_{\Delta T}$ ,  $\alpha_p$  depend in a nontrivial manner on the property relations of the two phases evaluated at  $T_s$ .

For the postulated local equilibrium of the interface the parentheses in (29) are unity, which yields an implicit equation for the interface temperature  $T_s$ ,

$$\frac{T_s - T_L}{T_s} = -\frac{\delta T_L}{T_s} = \bar{\alpha}_{\Delta T}(T_s) \frac{\Delta T}{T_s} - \bar{\alpha}_p(T_s) \frac{\delta p}{p_{\text{sat}}(T_s)} \quad (30)$$

with dimensionless coefficients  $\bar{\alpha}_{\Delta T} = \frac{\alpha_{\Delta T}}{\alpha_{T_L}}$ ,  $\bar{\alpha}_p = -\frac{\alpha_p}{\alpha_{T_L}}$ . This equation relates the difference between liquid and interface temperatures to the temperature jump between phases and the deviation from saturation pressure, which both can be measured in principle.

We consider two examples: (1) a van der Waals fluid, where dimensionless property relations read (temperature  $\tau$ , mass density  $\varrho$ ) [28],

$$\begin{aligned} p(\tau, \varrho) &= \frac{3\varrho\tau}{3-\varrho} - \frac{9}{8}\varrho^2, \quad u(\tau, \varrho) = \frac{3}{2}\tau - \frac{9}{8}\varrho, \\ s(\tau, \varrho) &= \frac{3}{2} \ln \tau + \ln \left( \frac{3}{\varrho} - 1 \right), \end{aligned} \quad (31)$$

made dimensionless such that  $\tau_{\text{crit}} = \varrho_{\text{crit}} = 1$  and  $p_{\text{crit}} = 0.375$ , so that  $Z_{\text{crit}} = \frac{p}{\rho\tau}|_{\text{crit}} = 0.375$ ; and (2) the Sutherland model (hard sphere repulsion and sixth-order attraction) combined with the Carnahan-Starling equation of state for hard sphere molecules, here in dimensionless form [27],

$$\begin{aligned} p(\tau, \varrho) &= \varrho\tau \left[ 1 + \frac{2\pi}{3} \varrho \frac{1 - \frac{\pi}{12}\varrho}{(1 - \frac{\pi}{6}\varrho)^3} \right] - \frac{4\pi}{3} \varrho^2, \\ u(\tau, \varrho) &= \frac{3}{2}\tau - \frac{4\pi}{3}\varrho, \\ s(\tau, \varrho) &= \frac{3}{2} \ln \tau - \ln \varrho - \frac{3 - \frac{\pi}{3}\varrho}{(1 - \frac{\pi}{6}\varrho)^2} \end{aligned} \quad (32)$$

with  $\tau_{\text{crit}} = 0.755$ ,  $\varrho_{\text{crit}} = 0.249$  and  $p_{\text{crit}} = 0.0675$ , so that  $Z_{\text{crit}} = \frac{p}{\rho\tau}|_{\text{crit}} = 0.359$ .

Figure 3 shows the pressure-density diagrams for both models, with the saturation lines determined from Maxwell's equal-area argument and three isothermal lines (subcritical, critical, and supercritical) [28].

The coefficients  $\bar{\alpha}_{\Delta T}$ ,  $\bar{\alpha}_p$  are shown in Fig. 4 on a logarithmic scale for dimensionless temperatures  $T/T_{\text{crit}}$  in (0.45, 1). The figure also shows the equilibrium density ratio  $\rho_V/\rho_L$ , which is of similar magnitude as the two coefficients.

Both coefficients  $\bar{\alpha}_{\Delta T}$ ,  $\bar{\alpha}_p$  are rather small for most temperatures, with the Carnahan-Starling-Sutherland model giving even smaller values than van der Waals. Based on these data Eq. (30) predicts temperature differences between the liquid temperature  $T_L$  and the postulated interface temperature  $T_s$  well below 10% of the liquid-vapor temperature jump  $\Delta T$  for most evaporation problems.

In other words, for states well below the critical point the interface temperature  $T_s$  is expected to deviate only a little from the extrapolated liquid temperature  $T_L$ . For many practical applications, such as the reported experiments which are conducted close to the triple point, it will suffice to set  $T_s = T_L$ .

For states closer to the critical point, say, for  $T/T_{\text{crit}} > 0.8$ , the models predict noticeable differences between liquid and interfacial temperatures.

### D. Remarks on surface tension and pressure

Surface tension is the result of anisotropic capillary stresses in the interfacial region. With viscous stresses ignored, we write the stress tensor in the interfacial region as

$$P_{ij} = p(\tilde{\rho}, \tilde{T}) \delta_{ij} + P_{ij}^K + \Pi_{ij}. \quad (33)$$

Here  $\tilde{\rho}(x)$ ,  $\tilde{T}(x)$  indicate fully resolved curves as in (10). The pressure  $p(\rho, T)$  follows a nonmonotonous equation of state; i.e., pressure is van der Waals-like. Dominant interfacial

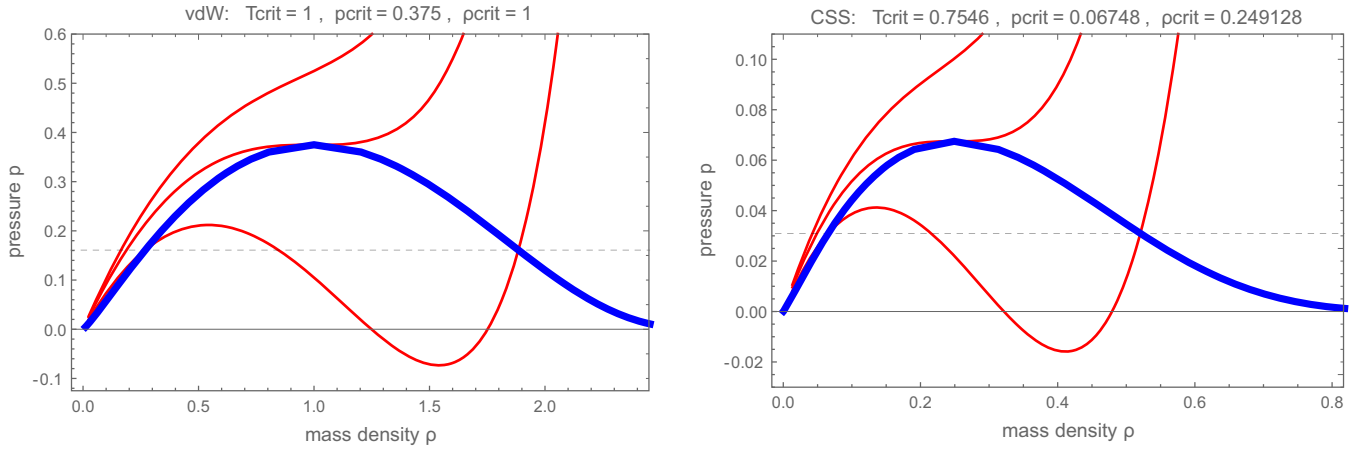


FIG. 3. Pressure density diagrams for van der Waals (left) and CSS (right), with saturation lines (blue) and three isothermal lines (red). The dashed horizontal line indicates the saturation pressure for the subcritical isotherm.

stresses are denoted by  $P_{ij}^K$ , for which one might think of Korteweg capillary stresses of the form [36]

$$P_{ij}^K = -\chi \left[ \left( \tilde{\rho} \frac{\partial^2 \tilde{\rho}}{\partial x_r \partial x_r} + \frac{1}{2} \frac{\partial \tilde{\rho}}{\partial x_r} \frac{\partial \tilde{\rho}}{\partial x_r} \right) \delta_{ij} - \frac{\partial \tilde{\rho}}{\partial x_i} \frac{\partial \tilde{\rho}}{\partial x_j} \right], \quad (34)$$

where  $\chi$  is a coefficient related to the interatomic potential. The Korteweg stress gives a reasonably realistic description of the interface in equilibrium, where temperature is constant  $\tilde{T}(x) = T$ , with the resulting density profile  $\tilde{\rho}_E(x)$ . In nonequilibrium, with mass and heat fluxes passing through the interface, the temperature in the interface will not be constant, but change on small scale, e.g., due to evaporative cooling effects and heat transfer. This will influence not only local pressures but also introduce nonequilibrium stresses  $\Pi_{ij}$ , such as thermal stresses. A proper local description of the interface requires a fully resolved energy balance and appropriate constitutive relations. Here is not the place to discuss details (see, e.g., [26,27]), but we can proceed formally.

The density profile  $\tilde{\rho}(x)$  results from solving the momentum balance in a normal direction

$$P_{xx} = p(\tilde{\rho}(x), \tilde{T}(x)) - \chi \left( \tilde{\rho} \frac{d^2 \tilde{\rho}}{dx^2} - \frac{1}{2} \frac{d\tilde{\rho}}{dx} \frac{d\tilde{\rho}}{dx} \right) + \Pi_{xx} = P_0, \quad (35)$$

where  $P_0$  is constant system pressure. In equilibrium with  $\tilde{T}(x) = T$  and  $\Pi_{ij} = 0$  we have  $P_0 = p_{\text{sat}}(T)$ , and the saturation pressure can be found from Maxwell's equal area rule, which also yields the bulk densities [28].

The gradient terms in  $P_{ij}^K$  and  $\Pi_{ij}$  compensate the unstable branch of the pressure curve  $p(\rho, T)$ . The surface tension results from the difference between normal and tangential stress as

$$\begin{aligned} \gamma &= \int_{-L}^L (P_{xx} - P_{zz}) dx \\ &= \chi \int_{-L}^L \left( \frac{d\tilde{\rho}}{dx} \right)^2 dx + \int_{-L}^L (\Pi_{xx} - \Pi_{zz}) dx. \end{aligned} \quad (36)$$

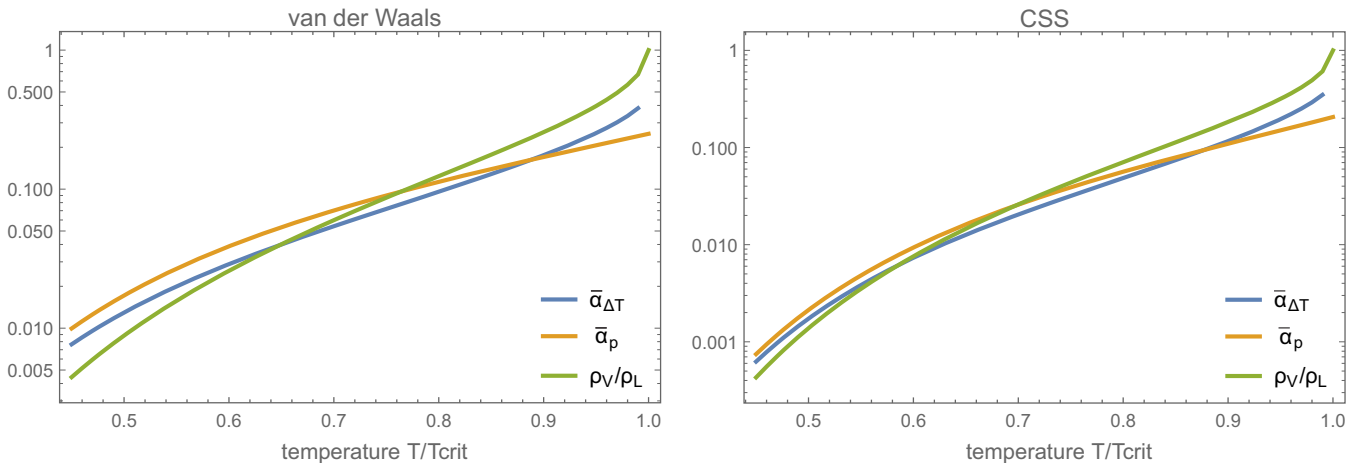


FIG. 4. Coefficients  $\bar{\alpha}_{\Delta T}$ ,  $\bar{\alpha}_p$  for determination of interface temperature, and liquid-vapor density ratio  $\rho_v/\rho_L$ , for van der Waals gas (vdW) and Carnahan-Starling-Sutherland gas (CSS).

From (35, 36) it is evident that nonequilibrium processes deform the interface ( $\tilde{\rho} \neq \tilde{\rho}_E$ ) and thus affect surface tension  $\gamma$ . The proposed interface temperature  $T_s^{(\gamma)} = \gamma_E^{-1}(\gamma)$  results from the deformation of the interface due to nonequilibrium effects and appearance of Knudsen layers. In contrast, the temperature  $T_s^{(\eta)} = T_s^{(\varepsilon)}$  from the Clausius-Clapeyron-type relations depends only on bulk properties. It appears quite unlikely that both should agree.

In a recent evaluation of a van der Waals fluid simulation data gave proof, both of the agreement of  $T_s^{(\eta)}$  and  $T_s^{(\varepsilon)}$  and of these being different from  $T_s^{(\gamma)}$  [32].

#### IV. EXTENDED INTERFACE THERMODYNAMICS: STRUCTURAL VARIABLE

##### A. Structural variables and gauge invariance

When the proposed interface temperatures different for stronger nonequilibrium,  $T_s^{(\gamma)} \neq T_s^{(\eta)}$ , the local equilibrium description of liquid-vapor interfaces does not succeed. In a phenomenological extension of the formalism, we add one or several structural (or internal) variables to the description of phase interfaces in nonequilibrium processes.

The structural variables are not specified in their physical meaning, but one might think of them as a measure of the influence of nonequilibrium transport of heat and mass across the interface, which leads to deformation of the interface (relative to the equilibrium) and other nonequilibrium effects, such as Knudsen layers.

In the light of [26,27], one might think of a moment system describing the bulk phases and the interface, where moments describing the contributions above hydrodynamics are rescaled such that they are zero in the hydrodynamic regime, and hence in the bulk phases. Within nonequilibrium interfaces, however, these higher order variables are nonzero. The structural variable(s) aims at giving a lump description of these nonequilibrium contributions in the interface.

The interfacial behavior could also be affected by the presence of surfactants that affect the mass and heat transfer properties of the interface. Then, the structural variable accounts for the presence and variation of surfactants; e.g., it could be chosen as deviation of surfactant density from an equilibrium value.

Adding one extensive structural variable  $\lambda_s$  with intensive partner  $\beta_s$ , the Gibbs, Euler, and Gibbs-Duhem (9, 8) relations are extended to read

$$\begin{aligned} T_s d\eta_s &= d\varepsilon_s - \mu_s d\rho_s - \beta_s d\lambda_s, \\ \mu_s \rho_s &= \varepsilon_s - T_s \eta_s - \gamma - \beta_s \lambda_s, \\ 0 &= -\eta_s dT_s - \rho_s d\mu_s - \lambda_s d\beta_s - d\gamma. \end{aligned} \quad (37)$$

Any number of structural variables can be added in the same manner; for the moment we write only one. Here  $\mu_s$  denotes the interface chemical potential in this setting, which in phase equilibrium reduces to  $\mu_s = \mu_E(T)$ . Moreover,  $\gamma$  is the surface tension of the nonequilibrium interface, which differs from the equilibrium value  $\gamma_E(T_s)$ .

The structural variable  $\lambda$  has no counterpart in the bulk, that is, outside the interfacial region  $\lambda = 0$ . With that,  $\Delta\lambda = 0$ , hence  $\lambda_s$  is gauge invariant by definition. The

requirement of gauge invariance of the Euler and Gibbs-Duhem equations (37)<sub>2,3</sub> yields

$$\Delta\varepsilon - T\Delta\eta - \mu_s\Delta\rho = 0, \quad 0 = -\Delta\eta dT_s - \Delta\rho d\mu_s, \quad (38)$$

which are just as before in (13) and (14), only that  $\gamma_E, \mu_E$  are replaced by  $\gamma, \mu_s$ .

The second relation (38) implies that the chemical potential  $\mu_s$  varies only with temperature  $T_s$ , so that also for this extended model the chemical potential of the interface is a function of interface temperature alone,  $\mu_s(T_s)$ . Then, to match the equilibrium limit, we must have

$$\mu_s(T_s) = \mu_E(T_s). \quad (39)$$

We thus find from (38) and (39) the same Clausius-Clapeyron equations for the nonequilibrium interface as without structural variable, where interface temperature  $T_s$  is defined as

$$\frac{\Delta\eta}{\Delta\rho} = -\left.\frac{d\mu_E}{dT}\right|_{T=T_s}, \quad \frac{\Delta\varepsilon}{\Delta\rho} = \left.\frac{d\frac{\mu_E}{T}}{d\frac{1}{T}}\right|_{T=T_s}. \quad (40)$$

We have seen already that these are compatible to each other, as long as we have first-order deviations from equilibrium saturation. For given bulk properties  $T_L, T_V, p$ , the above equations define a unique interface temperature  $T_s$ .

The Gibbs-Duhem relation (37)<sub>3</sub> provides information on surface tension as a function of interface temperature and the intensive structural variable  $\beta_s$ ,

$$d\gamma = -\left(\eta_s + \rho_s \frac{d\mu_E}{dT_s}\right) dT_s - \lambda_s d\beta_s; \quad (41)$$

that is, the nonequilibrium surface tension is a function of two variables,  $\gamma(T_s, \beta_s)$ . Surface tension can be considered as a thermodynamic potential [28], which gives entropy and structural variable by derivative,

$$\begin{aligned} \eta_s(T_s, \beta_s) &= -\left(\frac{\partial\gamma}{\partial T_s}\right)_{\beta_s} - \rho_s \frac{d\mu_E}{dT_s} \\ \lambda_s(T_s, \beta_s) &= -\left(\frac{\partial\gamma}{\partial\beta_s}\right)_{T_s}, \end{aligned} \quad (42)$$

while interface energy is obtained from this and the Euler equation as

$$\varepsilon_s(T_s, \beta_s) = \left(\frac{\partial\gamma}{\partial\frac{1}{T_s}}\right)_{\beta_s} + \rho_s \frac{d\frac{\mu_E}{T_s}}{d\frac{1}{T_s}} - \beta_s \left(\frac{\partial\gamma}{\partial\beta_s}\right)_{T_s}. \quad (43)$$

With the structural variable(s), the matching problem of the local equilibrium assumption, where  $T_s^{(\eta)}$  from  $\frac{\Delta\eta}{\Delta\rho} = -\frac{d\mu_E}{dT}$  and  $T_s^{(\gamma)} = \gamma_E^{-1}(\gamma)$  must agree, is avoided, and the difference between both temperatures is accommodated by the structural variable(s). While the interface temperature is defined through the (compatible) jump conditions (17)<sub>1,2</sub>, the surface tension now is a function of two variables and cannot be used to define interfacial temperature.

##### B. 1D transport model

We study transport of mass and energy across the interface, from the viewpoint of an observer resting with the interface. We denote mass flux as  $J$ , conductive heat flux as  $q$ , and total energy flux as  $Q = Jh + q$ , with enthalpy  $h = u + \frac{p}{\rho}$ . In the



1D model to be considered here, there is no transport along the interface, just exchange processes between the interface and the adjacent bulk phases; see Fig. 1.

We specifically consider the gauge  $\rho_s = 0$ , so that the interface cannot accumulate or lose mass. With mass and energy conserved, their interface values can change only due to exchange with the bulk phases, while the structural variable will be nonconserved. This gives the balance laws for mass, energy, and internal variables as

$$\begin{aligned} 0 &= J_L - J_V, \\ \frac{d\varepsilon_s}{dt} &= (J_L h_L + q_L) - (J_V h_V + q_V), \\ \frac{d\lambda_s}{dt} &= \pi_s, \end{aligned} \quad (44)$$

where the direction of transport from liquid to interface is chosen as positive. The first equation is the mass balance for the interface with  $\rho_s = 0$  fixed; conservation of mass thus implies

$$J_L = J_V = J. \quad (45)$$

The fluxes for energy follow directly from classical hydrodynamics at small Mach numbers in one dimension. In the balance for the internal variable,  $\pi_s$  describes the overall variation of the internal variable due to exchange with the bulk phases and interface processes.

The interface entropy changes due to flux exchange of entropy with the bulk phases, and internal production,

$$\frac{d\eta_s}{dt} = \left( J_L s_L + \frac{q_L}{T_L} \right) - \left( J_V s_V + \frac{q_V}{T_V} \right) + \Sigma_s, \quad (46)$$

where  $J_\alpha s_\alpha + \frac{q_\alpha}{T_\alpha}$  is the well-known convective plus conductive entropy flux entering or leaving the bulk phases, and  $\Sigma_s \geq 0$  is the entropy generation rate within the interface.

Use of the Gibbs equation for the interface (37)<sub>1</sub> and replacing time derivatives of the variables from the balance laws yield, after some reordering, the entropy generation rate as a sum of products of thermodynamic forces and fluxes,

$$\Sigma_s = F_J J + \mathcal{F}_{q_L} q_L + \mathcal{F}_{q_V} q_V + \mathcal{F}_{\pi_s} \pi_s, \quad (47)$$

where we introduce the thermodynamic forces

$$\begin{aligned} F_J &= \frac{1}{T_s} (h_L - h_V) - s_L + s_V, \\ \mathcal{F}_{q_L} &= \frac{1}{T_s} - \frac{1}{T_L}, \\ \mathcal{F}_{q_V} &= \frac{1}{T_V} - \frac{1}{T_s}, \\ \mathcal{F}_{\pi_s} &= -\frac{\beta_s}{T_s}. \end{aligned} \quad (48)$$

Thermodynamic forces measure the deviation from equilibrium. The forces vanish in equilibrium at  $T_s$ , where  $T_{\alpha|E} = T_s$ ,  $\mu_{\alpha|E} = \mu_E(T_s)$ ,  $\beta_{s|E} = 0$ .

The entropy generation rate (47) is the sum of products of the above thermodynamic forces and the corresponding thermodynamic fluxes  $J$ ,  $q_L$ ,  $q_V$ ,  $\pi_s$ , which drive the system towards equilibrium. To proceed, we use the ideas of linear irreversible thermodynamics (LIT) [2,19], which assumes linear relations between fluxes and forces. Accordingly, we write

the force-flux relations with symmetric and positive definite resistivity matrix  $\mathcal{R}_{AB}$ ,

$$\begin{bmatrix} F_J \\ \mathcal{F}_{q_L} \\ \mathcal{F}_{q_V} \\ \mathcal{F}_{\pi_s} \end{bmatrix} = \begin{bmatrix} \mathcal{R}_{JJ} & \mathcal{R}_{Jq_L} & \mathcal{R}_{Jq_V} & \mathcal{R}_{J\pi_s} \\ \mathcal{R}_{q_L J} & \mathcal{R}_{q_L q_L} & \mathcal{R}_{q_L q_V} & \mathcal{R}_{q_L \pi_s} \\ \mathcal{R}_{q_V J} & \mathcal{R}_{q_V q_L} & \mathcal{R}_{q_V q_V} & \mathcal{R}_{q_V \pi_s} \\ \mathcal{R}_{\pi_s J} & \mathcal{R}_{\pi_s q_L} & \mathcal{R}_{\pi_s q_V} & \mathcal{R}_{\pi_s \pi_s} \end{bmatrix} \begin{bmatrix} J \\ q_L \\ q_V \\ \pi_s \end{bmatrix}. \quad (49)$$

The phenomenological coefficients  $\mathcal{R}_{AB}$  must be determined either from experiment or from first principles. This is rather difficult, since one can evaluate the interfacial behavior only as part of a larger system, where the bulk behavior often overshadows the influence of the interfacial resistivities. As will be seen below, the number of coefficients can be significantly reduced (from ten to three) if one restricts the interest to steady state.

Combining the interface balance (44)<sub>3</sub> for  $\lambda_s$  with (48)<sub>4</sub> and the last line of (49) yields the balance for the internal variable as

$$\frac{d\lambda_s}{dt} = -\frac{\mathcal{R}_{J\pi_s}}{\mathcal{R}_{\pi_s \pi_s}} J - \frac{\mathcal{R}_{q_L \pi_s}}{\mathcal{R}_{\pi_s \pi_s}} q_L - \frac{\mathcal{R}_{q_V \pi_s}}{\mathcal{R}_{\pi_s \pi_s}} q_V - \frac{\beta_s}{\mathcal{R}_{\pi_s \pi_s} T_s}. \quad (50)$$

Here the terms with  $J$ ,  $q_L$ ,  $q_V$  describe production and destruction of structural variable by interplay between interface and bulk phases due to in- and outgoing fluxes of mass and energy, while the last term describes the production (positive or negative) of the structural variable within the interface.

### C. Steady state

With the interface thickness being rather small, one will expect that steady state is established fast relative to variations in a macroscopic process. Then it suffices to study the steady state of the interface, for which the balance equations (44) for energy and internal variable reduce to

$$q_L = J(h_V - h_L) + q_V, \quad \pi_s = 0. \quad (51)$$

With this, the entropy generation rate (47) simplifies to the well-known expression [2,3]

$$\Sigma_s^{\text{stst}} = \left[ \frac{\mu_L}{T_L} - \frac{\mu_V}{T_V} + \left( \frac{1}{T_V} - \frac{1}{T_L} \right) h_V \right] J + \left( \frac{1}{T_V} - \frac{1}{T_L} \right) q_V, \quad (52)$$

which gives rise to the phenomenological force-flux relations for the steady-state interface

$$\begin{aligned} \begin{bmatrix} \hat{\mathcal{F}}_J \\ \hat{\mathcal{F}}_{q_V} \end{bmatrix} &= \begin{bmatrix} \frac{\mu_L}{T_L} - \frac{\mu_V}{T_V} + \left( \frac{1}{T_V} - \frac{1}{T_L} \right) h_V \\ \frac{1}{T_V} - \frac{1}{T_L} \end{bmatrix} \\ &= \begin{bmatrix} \hat{\mathcal{R}}_{JJ} & \hat{\mathcal{R}}_{Jq_V} \\ \hat{\mathcal{R}}_{q_V J} & \hat{\mathcal{R}}_{q_V q_V} \end{bmatrix} \begin{bmatrix} J \\ q_V \end{bmatrix}. \end{aligned} \quad (53)$$

These force-flux relations are also obtained by linear combination of (49), which gives the steady-state resistivities  $\hat{\mathcal{R}}_{AB}$  in terms of the general resistivities  $\mathcal{R}_{AB}$  as

$$\begin{aligned} \hat{\mathcal{R}}_{JJ} &= \mathcal{R}_{JJ} + 2\mathcal{R}_{Jq_L}(h_V - h_L) + \mathcal{R}_{q_L q_L}(h_V - h_L)^2, \\ \hat{\mathcal{R}}_{Jq_V} &= \hat{\mathcal{R}}_{q_V J} = \mathcal{R}_{Jq_L} + \mathcal{R}_{Jq_V} + (\mathcal{R}_{q_L q_L} + \mathcal{R}_{q_L q_V})(h_V - h_L), \\ \hat{\mathcal{R}}_{q_V q_V} &= \mathcal{R}_{q_L q_L} + 2\mathcal{R}_{q_L q_V} + \mathcal{R}_{q_V q_V}. \end{aligned} \quad (54)$$

Notably, in steady state the equation for the structural variable is decoupled from the above; it reduces to

$$-\frac{\beta_s}{T_s} = \hat{\mathcal{R}}_{J\pi_s} J + \hat{\mathcal{R}}_{q_V\pi_s} q_V \quad (55)$$

with the combined resistivities

$$\hat{\mathcal{R}}_{J\pi_s} = \mathcal{R}_{J\pi_s} + \mathcal{R}_{q_L\pi_s}(h_V - h_L), \quad \hat{\mathcal{R}}_{q_V\pi_s} = \mathcal{R}_{q_V\pi_s} + \mathcal{R}_{q_L\pi_s}. \quad (56)$$

According to (55), the intensive structural variable  $\beta_s$  is induced by mass and heat transfer through the interface such that  $\beta_s$  vanishes in equilibrium and grows with the degree of nonequilibrium, which is induced by larger mass and heat fluxes.

Since the structural variable accounts for deviation of surface tension  $\gamma$  from its equilibrium value  $\gamma_E(T_s)$ , one will expect that this deviation grows with the degree of nonequilibrium.

#### D. Linear and nonlinear resistivities

We ask for the dependencies of the resistivities  $\mathcal{R}_{AB}$  and  $\hat{\mathcal{R}}_{AB}$  on the thermodynamic properties that describe the system and the processes.

Classically, LIT aims for strictly linear relations between fluxes and forces, and with the fluxes explicitly appearing on the right-hand side of Eq. (49), the coefficients should depend only on the interfacial local equilibrium state,

$$\text{LIT: } \mathcal{R}_{AB}(T_s), \quad \hat{\mathcal{R}}_{AB}(T_s). \quad (57)$$

When the modeling is extended to include a structural variable, the state of the interface is given by interface temperature  $T_s$  and the structural variable  $\beta_s$ ; hence one will expect dependence on both, so that

$$\text{LIT (with structural variable): } \mathcal{R}_{AB}(T_s, \beta_s), \quad \hat{\mathcal{R}}_{AB}(T_s, \beta_s).$$

In a more general examination, one might allow that the resistivities—most of which describe the interaction of interface with the neighboring bulk phases—depend not only on the actual state of the interface as given by  $(T_s, \beta_s)$ , but also on the state of the adjacent bulk phases, i.e., they depend on, e.g.,  $(T_s, \beta_s; T_L, T_V, p)$ , where  $p$  is the common pressure of both phases (low Mach number flow).

With temperatures and chemical potentials  $\mu_\alpha(T_\alpha, p)$  homogeneous in equilibrium, and the forces vanishing in equilibrium, the differences between the bulk variables  $(T_\alpha, \mu_\alpha)$  and the interface values  $(T_s, \mu_E(T_s))$  are given through the size of the forces  $(\mathcal{F}_J, \mathcal{F}_{q_L}, \mathcal{F}_{q_V})$  in (48),

$$\begin{aligned} &(T_s, \beta_s; T_L, T_V, p) \\ &\quad \Downarrow \\ &(T_s, \beta_s; \mathcal{F}_J, \mathcal{F}_{q_L}, \mathcal{F}_{q_V}). \end{aligned} \quad (58)$$

Note that  $\mathcal{F}_{\pi_s} = -\frac{\beta_s}{T_s}$  depends on the interfacial state and must not be listed.

Furthermore, by (49)<sub>1,2</sub> the forces are expressed through the fluxes  $(J, q_L, q_V, \pi_s)$ . Hence, we can consider yet another

equivalent lists of variables

$$\begin{aligned} &(T_s, \beta_s; \mathcal{F}_J, \mathcal{F}_{q_L}, \mathcal{F}_{q_V}) \\ &\quad \Downarrow \\ &(T_s, \beta_s; J, q_L, q_V). \end{aligned} \quad (59)$$

Note that the flux  $\pi_s$  does not appear, since it can be expressed through the other variables [ $\pi_s$  is equal to the right-hand side of the balance (50)].

In summary, we find that in the nonlinear case, the full set of resistivities can be considered as functions of the bulk fluxes, as

$$\text{nonlinear: } \mathcal{R}_{AB}(T_s, \beta_s; J, q_L, q_V). \quad (60)$$

For steady-state interfaces the list of variables is further reduced, since the heat flux in the liquid  $q_L$  is expressed by  $q_V$  and bulk properties through (51)<sub>1</sub>, and the internal variable  $\beta_s$  is induced by mass and energy flux (55), so that we find the nonlinear resistivities in the principal form

$$\text{nonlinear (steady state): } \hat{\mathcal{R}}_{AB}(T_s, J, q_V), \quad (61)$$

where the interface temperature  $T_s$  is determined from the bulk properties in nonequilibrium by means of (40).

As argued above, for most practical purposes the interfacial temperature is expected to be rather close to the temperature of the bulk liquid at the interface, hence one might use

$$\text{nonlinear (practical): } \hat{\mathcal{R}}_{AB}(T_L, J, q_V). \quad (62)$$

Nonlinear resistivities must be found either from exhaustive MD or DSMC simulations or from evaporation models. The Appendix presents a variant of the classical Hertz-Knudsen-Schrage model for ideal gas vapors, which exhibits nonlinear relations between thermodynamic fluxes and thermodynamic forces. Accordingly, this model will yield nonlinear resistivities when exploited for processes outside the linear regime. The evaluation of this model is currently in progress and will be presented elsewhere.

## V. CONCLUSIONS

The assumption of local thermodynamic equilibrium for phase interface introduces three different definitions for the interface temperature  $T_s$ : the temperatures  $T_s^{(\eta)}$  and  $T_s^{(\varepsilon)}$ , which are found from Clausius-Clapeyron jump conditions between liquid and vapor bulk properties, and the temperature  $T_s^{(\gamma)}$ , which is defined through the equilibrium relation between surface tension and temperature.

In this contribution we have shown that  $T_s^{(\eta)}$  and  $T_s^{(\varepsilon)}$  are identical as long as the differences between liquid and vapor properties are of first order, with values rather close to the temperature  $T_L$  of the bulk liquid in front of the interface. We argued that outside of equilibrium, the surface-tension-based temperature  $T_s^{(\gamma)}$  is not naturally linked to  $T_s^{(\eta)} = T_s^{(\varepsilon)}$ , and differences are expected.

Enhancing the thermodynamic description by structural variables, the definition of the temperatures  $T_s^{(\eta)}$  and  $T_s^{(\varepsilon)}$  remains unchanged, while the difference of these from  $T_s^{(\gamma)}$  is described by the structural variables.

Specifically, the structural variables describe nonlinear transport behavior, where mass and heat transfer resistivities

are functions not only of interface temperature  $T_i$  but as well of mass and heat fluxes. Quantification of the nonlinearities requires detailed models or microscopic simulations for evaluation, which will help to clarify the question whether, e.g., molecular dynamics simulations in strong nonequilibrium are performed outside the linear regime.

#### ACKNOWLEDGMENTS

This paper presents results obtained during H.S.'s stimulating long-term visit to the group of H.C.O. at ETH Zürich in 2023. H.S. acknowledges support from ETH and the Natural Sciences and Engineering Research Council of Canada

(NSERC) through Discovery Grant No. RGPIN-2022-03188. H.C.O. is grateful to ETH Zürich for continued support after retirement.

#### APPENDIX: HERTZ-KNUDSEN-SCHRAGE MODEL AS EXAMPLE OF NONLINEAR INTERFACE BEHAVIOR

A simple Hertz-Knudsen-Schrage model for an ideal gas vapor and incompressible liquid based on a Maxwell interface model with condensation coefficient  $\psi$  and accommodation coefficient  $\gamma$  yields mass and heat fluxes as nonlinear functions of the liquid and vapor temperatures at the sharp interface as [3]

$$J = \frac{2\psi}{2-\psi} \left[ \frac{p_{\text{sat}}(T_L)}{\sqrt{2\pi RT_L}} - \frac{p}{\sqrt{2\pi RT_V}} \right], \quad (\text{A1})$$

$$q_V = \frac{2\psi}{2-\psi} \left( 2RT_L - \frac{5}{2}RT_V \right) \left[ \frac{p_{\text{sat}}(T_L)}{\sqrt{2\pi RT_L}} - \frac{p}{\sqrt{2\pi RT_V}} \right] + \frac{4[\psi(1-\gamma) + \gamma]}{2-\psi(1-\gamma) - \gamma} \frac{p[RT_L - RT_V]}{\sqrt{2\pi RT_V}}. \quad (\text{A2})$$

These equations were obtained from simplifying assumptions as discussed in [3], most notably the ignorance of Knudsen layers. This model corresponds to the steady-state relations (53).

The fluxes (A1) and (A2) are given in terms of bulk properties  $T_L$ ,  $T_V$ ,  $p$  at the interface. For evaluation of the nonlinearity between thermodynamic forces and fluxes, we must replace the bulk properties through the forces. With the well-known property relations for the ideal gas the forces are identified as

$$\begin{bmatrix} \hat{\mathcal{F}}_J \\ \hat{\mathcal{F}}_{q_V} \end{bmatrix} = \begin{bmatrix} s_V - s_L - \frac{h_V - h_L}{T_L} \\ \frac{1}{T_V} - \frac{1}{T_L} \end{bmatrix} = \begin{bmatrix} c_p \left( 1 - \frac{T_V}{T_L} + \ln \frac{T_V}{T_L} \right) - R \ln \frac{p}{p_{\text{sat}}(T_L)} \\ \frac{1}{T_V} - \frac{1}{T_L} \end{bmatrix}. \quad (\text{A3})$$

Elimination of vapor temperature  $T_V$  and system pressure  $p$  gives the fluxes ( $J$ ,  $q_V$ ) as explicit nonlinear functions of the forces ( $\hat{\mathcal{F}}_J$ ,  $\hat{\mathcal{F}}_{q_V}$ ) and the temperature of the liquid at the interface,  $T_L$ ,

$$\frac{\sqrt{2\pi RT_L}}{p_{\text{sat}}(T_L)} J = \left\{ \frac{2\psi}{2-\psi} \left[ 1 - \sqrt{1 + (T_L \hat{\mathcal{F}}_{q_V})} \frac{\exp \left( \frac{c_p}{R} \left\{ \frac{(T_L \hat{\mathcal{F}}_{q_V})}{1 + (T_L \hat{\mathcal{F}}_{q_V})} - \ln [1 + (T_L \hat{\mathcal{F}}_{q_V})] \right\} \right)}{\exp \left[ \left( \frac{\hat{\mathcal{F}}_J}{R} \right) \right]} \right] \right\}, \quad (\text{A4})$$

$$\begin{aligned} \frac{\sqrt{2\pi RT_L}}{p_{\text{sat}}(T_L)} \frac{q_V}{RT_L} &= \left( -\frac{2\psi}{2-\psi} \frac{\frac{1}{2} - 2(T_L \hat{\mathcal{F}}_{q_V})}{1 + (T_L \hat{\mathcal{F}}_{q_V})} \right. \\ &\quad \left. + \left\{ \frac{\psi}{2-\psi} + \left[ \frac{4(\psi(1-\gamma) + \gamma)}{2-\psi(1-\gamma) - \gamma} - \frac{4\psi}{2-\psi} \right] (T_L \hat{\mathcal{F}}_{q_V}) \right\} \frac{\exp \left\{ \frac{c_p}{R} \left( \frac{(T_L \hat{\mathcal{F}}_{q_V})}{1 + (T_L \hat{\mathcal{F}}_{q_V})} - \ln [1 + (T_L \hat{\mathcal{F}}_{q_V})] \right) \right\}}{\sqrt{1 + (T_L \hat{\mathcal{F}}_{q_V})} \exp \left[ \left( \frac{\hat{\mathcal{F}}_J}{R} \right) \right]} \right). \quad (\text{A5}) \end{aligned}$$

Linear force-flux relations are obtained under the assumption of small forces (which imply small fluxes), where Taylor expansion to first order gives

$$\begin{bmatrix} \frac{\sqrt{2\pi RT_L}}{p_{\text{sat}}(T_L)} J \\ \frac{\sqrt{2\pi RT_L}}{p_{\text{sat}}(T_L)} \frac{q_V}{RT_L} \end{bmatrix} = \begin{bmatrix} \frac{2\psi}{2-\psi} & -\frac{\psi}{2-\psi} \\ -\frac{\psi}{2-\psi} & \left[ \frac{1}{2} \frac{\psi}{2-\psi} + \frac{4[\psi(1-\gamma) + \gamma]}{2-\psi(1-\gamma) - \gamma} \right] \end{bmatrix} \begin{bmatrix} \frac{\hat{\mathcal{F}}_J}{R} \\ T_L \hat{\mathcal{F}}_{q_V} \end{bmatrix}. \quad (\text{A6})$$

The equations are written such that the matrix of coefficients is the inverse of the matrix of dimensionless resistivities, which thus are

$$\hat{r}_{\alpha\beta}^{KT} = \begin{bmatrix} \frac{1}{\psi} - \frac{7}{16} \frac{1 - \frac{2}{7}(1-\gamma)(1-\psi)}{\gamma + \psi(1-\gamma)} & \frac{1}{8} \frac{2-\gamma-\psi(1-\gamma)}{\gamma + \psi(1-\gamma)} \\ \frac{1}{8} \frac{2-\gamma-\psi(1-\gamma)}{\gamma + \psi(1-\gamma)} & \frac{1}{4} \frac{2-\gamma-\psi(1-\gamma)}{\gamma + \psi(1-\gamma)} \end{bmatrix}. \quad (\text{A7})$$

For full accommodation ( $\gamma = 1$ ) these reduce further to

$$\hat{r}_{\alpha\beta}^{KT} = \begin{bmatrix} \frac{1}{\psi} - \frac{7}{16} & \frac{1}{8} \\ \frac{1}{8} & \frac{1}{4} \end{bmatrix}. \quad (\text{A8})$$

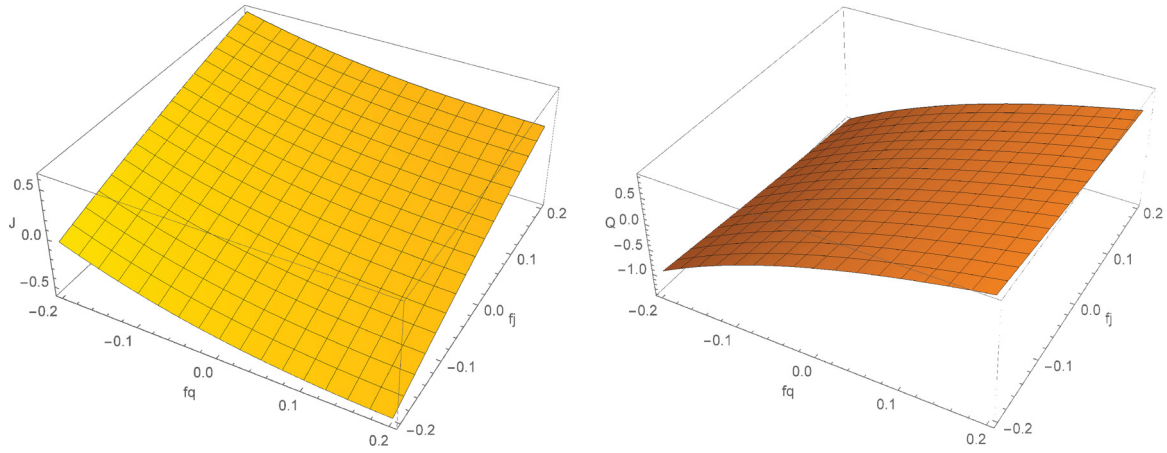


FIG. 5. Dimensionless mass and heat fluxes  $\hat{j}$ ,  $\hat{q}$  as functions of the dimensionless forces  $f_j$ ,  $f_q$  for the Hertz-Knudsen-Schrage model (A1) and (A2) with  $\psi = \gamma = 1$ .

Due to simplifications in the derivation, in particular ignorance of Knudsen layers, these differ slightly from the resistivities that can be extracted from the literature [1],

$$\hat{r}_{\alpha\beta}^{\text{Cipolla}} = \begin{bmatrix} \frac{1}{\psi} - 0.40044 & 0.126 \\ 0.126 & 0.2905 \end{bmatrix}. \quad (\text{A9})$$

With this principal agreement of the model in the linear regime, it is a natural conjecture that the underlying kinetic model will yield nonlinear resistivities for stronger nonequilibrium. While we will not further evaluate these force-flux

relations here, Fig. 5 shows the rescaled dimensionless fluxes

$$\hat{j} = \frac{\sqrt{2\pi RT_L}}{p_{\text{sat}}(T_L)} J, \quad \hat{q} = \frac{\sqrt{2\pi RT_L}}{p_{\text{sat}}(T_L)} \frac{q_V}{RT_L} \quad (\text{A10})$$

as a function of the dimensionless forces

$$f_j = \frac{\hat{F}_J}{R}, \quad f_q = T_L \hat{F}_{q_V}. \quad (\text{A11})$$

The nonlinear behavior is clearly visible for the chosen range of parameters. A more detailed evaluation of the nonlinear behavior and the corresponding resistivities is planned for the future.

- 
- [1] J. W. Cipolla, H. Lang, and S. K. Loyalka, Kinetic theory of condensation and evaporation. II, *J. Chem. Phys.* **61**, 69 (1974).
  - [2] S. Kjelstrup and D. Bedeaux, *Non-Equilibrium Thermodynamics of Heterogeneous Systems* (World Scientific, Singapore, 2008).
  - [3] J. P. Caputa and H. Struchtrup, Interface model for non-equilibrium evaporation, *Physica A* **390**, 31 (2011).
  - [4] I. Eames, N. Marr, and H. Sabir, The evaporation coefficient of water: A review, *Int. J. Heat Mass Transfer* **40**, 2963 (1997).
  - [5] R. Marek and J. Straub, Analysis of the evaporation coefficient and the condensation coefficient of water, *Int. J. Heat Mass Transfer* **44**, 39 (2001).
  - [6] G. Fang and C. A. Ward, Temperature measured close to the interface of an evaporating liquid, *Phys. Rev. E* **59**, 417 (1999).
  - [7] M. A. Kazemi and C. A. Ward, Assessment of the statistical rate theory expression for evaporation mass flux, *Int. J. Heat Mass Transfer* **179**, 121709 (2021).
  - [8] M. T. Rauter, A. Aasen, S. Kjelstrup, and Ø. Wilhelmsen, A comparative study of experiments and theories on steady-state evaporation of water, *Chem. Thermodyn. Thermal Anal.* **8**, 100091 (2022).
  - [9] R. Meland, A. Frezzotti, T. Ytrehus, and B. Hafskjold, Nonequilibrium molecular-dynamics simulation of net evaporation and net condensation, and evaluation of the gas-kinetic boundary condition at the interphase, *Phys. Fluids* **16**, 223 (2004).
  - [10] J. Xu, S. Kjelstrup, D. Bedeaux, A. Røsjorde, and L. Rekvig, Verification of Onsager's reciprocal relations for evaporation and condensation using non-equilibrium molecular dynamics, *J. Colloid Interface Sci.* **299**, 452 (2006).
  - [11] M. Schweizer, H. C. Öttinger, and T. Savin, Nonequilibrium thermodynamics of an interface, *Phys. Rev. E* **93**, 052803 (2016).
  - [12] P. Barbante and A. Frezzotti, A comparison of models for the evaporation of the Lennard-Jones fluid, *Eur. J. Mech. B Fluids* **64**, 69 (2017).
  - [13] M. Heinen and J. Vrabec, Evaporation sampled by stationary molecular dynamics simulation, *J. Chem. Phys.* **151**, 044704 (2019).
  - [14] S. Homes, M. Heinen, J. Vrabec, and J. Fischer, Evaporation driven by conductive heat transport, *Mol. Phys.* **119**, e1836410 (2021).
  - [15] A. Frezzotti and P. Barbante, Simulation of shock induced vapor condensation flows in the Lennard-Jones fluid by microscopic and continuum models, *Phys. Fluids* **32**, 122106 (2020).
  - [16] Ph. M. Rauscher, H. C. Öttinger, and J. de Pablo, Nonequilibrium statistical thermodynamics of multicomponent interfaces, *Proc. Natl. Acad. Sci. USA* **119**, e2121405119 (2022).

- [17] E. Johannessen and D. Bedeaux, The nonequilibrium van der Waals square gradient model. (II). Local equilibrium of the Gibbs surface, *Physica A* **330**, 354 (2003).
- [18] T. Savin, K. S. Glavatskiy, S. Kjelstrup, H. C. Öttinger, and D. Bedeaux, Local equilibrium of the Gibbs interface in two-phase systems, *Europhys. Lett.* **97**, 40002 (2012).
- [19] D. C. Venerus and H. C. Öttinger, *A Modern Course in Transport Phenomena* (Cambridge University Press, Cambridge, 2018).
- [20] D. Bedeaux, E. Johannessen, and A. Røsjorde, The nonequilibrium van der Waals square gradient model. (I). The model and its numerical solution, *Physica A* **330**, 329 (2003).
- [21] H. Hertz, Über die Verdunstung der Flüssigkeiten, insbesondere des Quecksilbers, im luftleeren Raume, *Ann. Phys.-Berlin* **253**, 177 (1882).
- [22] M. Knudsen, Die maximale Verdampfungsgeschwindigkeit des Quecksilbers, *Ann. Phys.-Berlin* **352**, 697 (1915).
- [23] R. W. Schrage, *A Theoretical Study of Interphase Mass Transfer* (Columbia University Press, New York, 1953).
- [24] M. Bond and H. Struchtrup, Mean evaporation and condensation coefficients based on energy dependent condensation probability, *Phys. Rev. E* **70**, 061605 (2004).
- [25] A. H. Persad and C. A. Ward, Expressions for the evaporation and condensation coefficients in the Hertz-Knudsen relation, *Chem. Rev.* **116**, 7727 (2016).
- [26] H. Struchtrup and A. Frezzotti, Twenty-six moment equations for the Enskog–Vlasov equation, *J. Fluid Mech.* **940**, A40 (2022).
- [27] H. Struchtrup, H. Jahandideh, A. Couteau, and A. Frezzotti, Heat transfer and evaporation processes from the Enskog–Vlasov equation, and its moment equations (unpublished).
- [28] H. Struchtrup, *Thermodynamics and Energy Conversion* (Springer, Heidelberg, 2014).
- [29] R. Evans, J. R. Henderson, D. C. Hoyle, A. O. Parry, and Z. A. Sabeur, Asymptotic decay of liquid structure: Oscillatory liquid–vapour density profiles and the Fisher–Widom line, *Mol. Phys.* **80**, 755 (1993).
- [30] P. Tarazona, E. Chacón, M. Reinaldo-Falagán, and E. Velasco, Layering structures at free liquid surfaces: The Fisher–Widom line and the capillary waves, *J. Chem. Phys.* **117**, 3941 (2002).
- [31] P. Mausbach, R. Fingerhut, and J. Vrabec, Thermodynamic metric geometry and the Fisher–Widom line of simple fluids, *Phys. Rev. E* **106**, 034136 (2022).
- [32] V. Klika and H. C. Öttinger, On the adequacy of bulk thermodynamics for thermodynamics of interfaces, *Multiscale Model. Simul.* (2023) (to be published).
- [33] P. Chomaz and F. Gulminelli, The challenges of finite-system statistical mechanics, *Eur. Phys. J. A* **30**, 317 (2006).
- [34] H. C. Öttinger, On small local equilibrium systems, *J. Non-Eq. Thermodyn.* **48**, 149 (2023).
- [35] H. Struchtrup, *Macroscopic Transport Equations for Rarefied Gas Flows* (Springer, Berlin, 2005).
- [36] D. M. Anderson, G. B. McFadden, and A. A. Wheeler, Diffusive-interface methods in fluid mechanics, *Annu. Rev. Fluid Mech.* **30**, 139 (1998).